Received: 3 May 2020 | Revised: 19 July 2020 | Accepted: 12 September 2020

DOI: 10.1002/qre.2785

RESEARCH ARTICLE

WILEY

Efficient monitoring of coefficient of variation with an application to chemical reactor process

Tahir Mahmood[1] | **Saddam Akber Abbasi**[2]

[1] Department of Technology, School of Science and Technology, The Open University of Hong Kong, Hong Kong, Hong Kong

[2] Department of Mathematics, Statistics, and Physics, Qatar University, Doha, Qatar

Correspondence
Saddam Akber Abbasi, Department of Mathematics, Statistics, and Physics, Qatar University, Doha, Qatar.
Email: sabbasi@qu.edu.qa; saddamabbasi@yahoo.com

Abstract

Control chart is a useful tool to monitor the performance of the industrial or production processes. Control charts are mostly adopted to detect unfavorable variations in process location (mean) and dispersion (standard deviation) parameters. In the literature, many control charts are designed for the monitoring of process variability under the assumption that the process mean is constant over time and the standard deviation is independent of the mean. However, for many real-life processes, the standard deviation may be proportional to mean, and hence it is more appropriate to monitor the process coefficient of variation (CV). In this study, we are proposing a design structure of the Shewhart type CV control chart under neoteric ranked set sampling with an aim to improve the detection ability of the usual CV chart. A comprehensive simulation study is conducted to evaluate the performance of the proposed $CV_{[\mathrm{NRSS}]}$ chart in terms of ARL, $MDRL$, and $SDRL$ measures. Moreover, the comparison of $CV_{[\mathrm{NRSS}]}$ chart is made with the existing competitive charts, based on simple random sampling, ranked set sampling (RSS), median RSS, and extreme RSS schemes. The results revealed that the proposed chart has better detection ability as compared to all existing competitive charts. Finally, a real-life example is presented to illustrate the working of the newly proposed CV chart.

KEYWORDS

coefficient of variation, control chart, neoteric ranked set sampling, run length, statistical process control

1 | INTRODUCTION

Production lines are the backbone of the industry, which are regularly monitored to ensure low production cost. To be competitive, companies utilize cost-efficient strategies and monitoring methods with an aim to maximize their profit and to exploit their production systems rationally. Most of the industries use statistical process control (SPC) tool-kit to monitor and control their production lines. The control chart is a widely used SPC tool, which provides online monitoring of a process. A traditional control chart comprises of two decision lines, namely, the lower control limit (LCL) and the upper

control limit (UCL). When the measurement of a quality characteristic falls outside of the decision lines, the production process is alarmed with an indication of the production of nonconforming items.

In the literature, most control chart structures are designed to monitor the location or dispersion parameter of the process. The Shewhart $\bar{X}$ chart and the median chart are popular charts for monitoring process location Montgomery,[1] and other location-based Shewhart charts are discussed in Schoonhoven et al[2] and Nazir et al.[3] The Shewhart charts based on the dispersion parameters are presented in Abbasi and Miller,[4] Ali et al,[5] Abbas et al,[6] and references therein. The location-based charts were designed under the assumption of equal variances. However, such assumption is not realistic. Therefore, joint or simultaneous structures of these charts were proposed, in which two charts were embedded together in such a way that one monitors the location parameter and other monitors dispersion parameter. The $\bar{X} - R$ and $\bar{X} - S$ charts are the basic simultaneous structures, while other simultaneous structures are discussed in Mahmood et al,[7] Zafar et al,[8] Sanusi et al,[9] and references therein.

Mostly in control chart settings, it is assumed that the process mean is stable over time, and the standard deviation is independent of the mean. However, such assumptions may not be valid for many real-life processes. Under these circumstances, it is recommended to monitor the coefficient of variation (CV). The CV-based chart was initially proposed by Kang et al[10] that involves plotting the sample CV (i.e., $W = S/\bar{X}$), where S and $\bar{X}$ represent the sample standard deviation and sample mean, respectively.

In the last few years, many CV control charts were proposed in the SPC literature. For instance, Connett and Lee[11] utilized a CV chart in the clinical trials to monitor split specimens of urine. Hong et al[12] provided an exponentially weighted moving average (EWMA) chart for the monitoring of process CV. The variance and CV charts based on their predictive distributions were designed by Menzefricke.[13] Castagliola et al[14] proposed two one-sided EWMA charts for monitoring the square of CV statistics, while this proposal is modified by Zhang et al[15] to enhance the sensitivity of EWMA charts. For efficient detection of the small shifts in the process, the double EWMA-based CV chart was proposed by Hong et al.[16] Further, the synthetic version of the CV chart was designed by Calzada and Scariano,[17] and run-rules with Shewhart CV chart were implemented by Castagliola et al.[18]

The one-sided Shewhart chart for the monitoring of process CV under short production runs was investigated by Castagliola et al,[19] and the economic design of the CV chart was discussed by Yeong et al.[20] Similar to the proposal of Castagliola et al,[14] the cumulative sum (CUSUM) structure was proposed by Tran and Tran.[21] Further, a side sensitive group runs chart for the monitoring of CV was proposed by You et al.[22] The CV control chart with variable sampling interval (VSI) strategy, variable sample size (VSS) strategy, and the combination of these two strategies was studied by Castagliola et al,[23] Castagliola et al,[24] Amdouni et al,[25] Amdouni et al,[26] Khaw et al,[27] Yeong et al,[28] and Muhammad et al.[29] Furthermore, the one-sided CV control chart under the measurement errors was proposed by Yeong et al,[30] and a Bayesian CV control chart was discussed by Van Zyl and Van der Merwe.[31]

All of the studies mentioned above have considered zero-state performance, while for the steady-state performance, Teoh et al[32] designed a chart, namely, the run-sum chart for the monitoring of process CV. The multivariate extension of the CV chart under zero-state structure was proposed by Yeong et al,[33] while under the steady-state structure was designed by Lim et al.[34] The one-sided synthetic version of CV chart with measurement errors was discussed by Tran et al,[35] and the ARL-unbiased Shewhart CV chart was proposed by Guo and Wang.[36] The adaptive version of multivariate CV chart with VSS and VSI strategies was proposed by Khaw et al,[37] while the phase I properties of univariate and multivariate CV chart were studied by Dawod et al,[38] and Abbasi and Adegoke.[39]

The CV control chart under repetitive group sampling plan was discussed by Yan et al,[40] under multiple repetitive group sampling plan was designed by Yan et al,[41] and under the double sampling plan was proposed by Ng et al.[42] The optimal design of EWMA-based CV chart was proposed by Teoh et al,[43] and a new EWMA chart for the monitoring of CV was proposed by Zhang et al.[44] This new EWMA-based CV chart was designed such that negative normalized observations of traditional CV-EWMA statistic were set at zero. By this modification, the new chart has better detection ability as compared to the conventional CV-based EWMA chart. Recently, Du Nguyen et al[45] studied Shewhart CV control chart with VSI strategy under measurement errors. The variable parameter chart for the monitoring of the univariate CV was discussed by Yeong et al,[46] and multivariate CV chart was proposed by Chew et al.[47] The one-sided CV control chart for the multivariate CV under short production runs was proposed by Khatun et al.[48]

Most of the studies mentioned above were designed under the simple random sampling (SRS) structure. However, ranked set sampling (RSS) structure proposed by McIntyre[49] is a more efficient sampling structure as compared to the SRS. Abbasi et al[50] proposed Shewhart CV chart under RSS and its modified strategies, and the EWMA-based CV chart under RSS schemes was designed by Noor-ul-Amin and Riaz.[51] Recently, Zamanzade and Al-Omari[52] proposed a new

ranked set scheme, namely, neoteric ranked set sampling (NRSS). The NRSS is a more efficient sampling structure as compared to the SRS and RSS schemes. Recent control charting structures under NRSS scheme may be found in Nawaz et al,[53] Nawaz and Han,[54] Abbas et al,[55] Hussain et al,[56] and references therein. In the literature, the Shewhart CV chart is not designed under the NRSS scheme, in the best of our knowledge. Hence, this study is intended to propose a Shewhart CV chart under the NRSS structure to obtain an efficient method for the monitoring of process CV. Further, the proposed structure is compared with the Shewhart CV chart under the SRS scheme Kang et al[10] and RSS strategies Abbasi et al.[50]

Rest of the article is organized as follows: the design structure of the proposed study is given in Section 2. Section 3 presents the performance evaluation of the proposed charts, while simulation study results and discussions are provided in Section 4. Section 5 consists of a real-life example to illustrate the working of new control chart, and finally, the conclusions and recommendations are reported in Section 6.

2 | THE DESIGN STRUCTURE OF THE PROPOSED STUDY

This section is designed to present different sampling schemes and the structure of the proposed CV chart.

2.1 | Sampling strategies

The choice of sampling scheme plays a significant role in decision making. In the SPC literature, control charts are designed under several sampling schemes, such as SRS, RSS, median RSS, extreme RSS, and so on. The SRS is the most straightforward sampling mechanism, in which all units in the population have an equal probability of being selected in a sample. Further, the description of RSS and NRSS methods is given in the following subsections.

2.1.1 | Ranked set sampling schemes

The structure of RSS was initiated by McIntyre.[49] The method of RSS is outlined as follows: draw n^2 (X, Z) samples from a bivariate normal distribution using specified correlation ρ and divide them into n sets having n observations in each set. In each set, actual observations (X) are ranked (in ascending order) according to the concomitant variable (Z). For actual RSS observations of size n, choose the first smallest actual observation from first set, second smallest actual observation from second set, and continue this procedure until the largest actual observation is selected from the n^{th} set.

The median RSS (MRSS) was introduced by Muttlak,[57] and its structure can be defined as follows: draw n^2 (X, Z) samples from a bivariate normal distribution using specified correlation ρ and divide them into n sets having n observations in each set. In each set, actual observations (X) are ranked (in ascending order) according to the concomitant variable (Z). For actual MRSS observations of size n, when the size of the set is even, choose half observations from the first $(n/2)$ sets and other from the last $((n + 2)/2)$ sets. However, when the size of the set is odd, select $((n + 1)/2)$ observations from each set.

Samawi et al[58] introduced another RSS scheme, namely, extreme RSS (ERSS). The mechanism of ERSS is defined as follows: draw n^2 (X, Z) samples from a bivariate normal distribution using specified correlation ρ and divide them into n sets having n observations in each set. In each set, actual observations (X) are ranked (in ascending order) according to the concomitant variable (Z). For actual ERSS observations of size n, when the size of the set is even, choose the smallest ranked observations of first $(n/2)$ sets and remaining were selected as the largest ranked observations of last $(n/2)$ sets. However, when the size of the set is odd, select the smallest sample from the first $((n - 1)/2)$ sets, largest sample from last $((n - 1)/2)$ sets, and the median of the rest of the sets.

2.1.2 | Neoteric ranked set sampling

Recently, Zamanzade and Al-Omari[52] proposed a new RSS scheme, namely, the NRSS. They showed that the NRSS scheme provides efficient estimates as compared to the SRS, RSS, MRSS, and ERSS schemes. The structure of NRSS

is described as follows: draw n^2 (X, Z) samples from a bivariate normal distribution using specified correlation ρ and divide them into n sets having n observations in each set. In each set, actual observations (X) are ranked (in ascending order) according to the concomitant variable (Z). For actual NRSS observations of size n, when the size of the set is odd, select $((n+1/2)+\ (k-1)n)^{th}$ ranked observations for $k = 1, 2, \dots, n$. However, when the size of the set is even, select $(h+\ (k-1)n)^{th}$ ranked observations, where $h = n/2$ when k is even, while $h = (n+2)/2$ when k is odd. Simplification of the above-mentioned procedure is obtained by selecting $X_{((n+1)/2)}, X_{((3n+1)/2)}, X_{((5n+1)/2)}, \dots, X_{((2n^2-n+1)/2)}$ ranked samples when the size of the set is even, while for the odd set size, select $X_{((n+2)/2)}, X_{((3n+2)/2)}, X_{((5n+2)/2)}, \dots, X_{((2n^2-n)/2)}$ ranked samples.

It is noted that all above-mentioned sampling strategies are further represented by $\aleph$. For example, if $\aleph = SRS$, then the samples are drawn by SRS. Similarly, $\aleph = RSS$ represents ranked set sampling, $\aleph = MRSS$ represents median ranked set sampling, $\aleph = ERSS$ represents extreme ranked set sampling, and $\aleph = NRSS$ is used for the NRSS. It is also to be noted that when $\rho = 1$, then all RSS strategies are categorized as perfect ranked set scheme; otherwise, imperfect ranked set scheme (i.e., $\rho \neq 1$).

2.2 | The $CV_{[\aleph]}$ charts

Let X represents a quality characteristic of interest having mean μ_X and standard deviation σ_X. The process CV (γ) can be defined as:

$$\gamma = \frac{\sigma_X}{\mu_X}. \tag{1}$$

The CV given in (1) is a standardized measure of the dispersion of X and has several benefits over the other measures of the dispersion, such as σ_X, which is always understood in the context of μ_X. Usually, parameters μ_X and σ_X are unknown and are estimated from the sample observations, where S and $\bar{X}$ represent the sample standard deviation and sample mean, respectively.

Assume $X_{ij[\aleph]}$ is the observed variable where sample number is indexed with $j; j = 1, 2, \dots, n$ and time is indexed with $i; i = 1, 2, \dots,$ for the sampling scheme $\aleph$. Hence, the i^{th} estimated CV statistic can be defined as follows:

$$W_{i[\aleph]} = \frac{S_{i[\aleph]}}{\bar{X}_{i[\aleph]}}, \tag{2}$$

where $\bar{X}_{i[\aleph]}$ is the sample mean, and $S_{i[\aleph]}$ is the sample standard deviation under $\aleph$ sampling scheme for the i^{th} sample. Let $L_{i[\aleph]} = W_{i[\aleph]}/\gamma$ be a pivotal quantity, which describes a link between the estimated and the population CV, and then the expected value of the pivotal quantity can be obtained by $E(L_{i[\aleph]}) = E\ (W_{i[\aleph]}/\gamma) = \bar{W}_{[\aleph]}/\gamma$. Assume $E(L_{i[\aleph]}) = k_{2[\aleph]}$, where, $k_{2[\aleph]}$ depends on n for a specific sampling scheme $\aleph$. Hence, the unbiased estimator of γ for the i^{th} sample can be defined as follows:

$$\hat{\gamma}_{i[\aleph]} = \frac{\bar{W}_{[\aleph]}}{k_{2[\aleph]}}. \tag{3}$$

The probability limits are considered as the decision lines for $CV_{[\aleph]}$ chart, which is defined on the base of the prespecified probability of a type I error α as follows:

$$\begin{aligned} LCL_{[\aleph]} &= L_{i[\aleph]\left(\frac{\alpha}{2}\right)}\frac{\bar{W}_{[\aleph]}}{k_{2[\aleph]}}, \quad \text{with } P\left(L_{i[\aleph]} \leq L_{i[\aleph]\left(\frac{\alpha}{2}\right)}\right) = \frac{\alpha}{2} \\ UCL_{[\aleph]} &= L_{i[\aleph]\left(1-\frac{\alpha}{2}\right)}\frac{\bar{W}_{[\aleph]}}{k_{2[\aleph]}}, \quad \text{with } P\left(L_{i[\aleph]} \geq L_{i[\aleph]\left(\frac{\alpha}{2}\right)}\right) = 1-\frac{\alpha}{2}. \end{aligned} \tag{4}$$

Hence, the values of plotting statistic $\hat{\gamma}_{[\aleph]}$ are plotted against $LCL_{[\aleph]}$ and $UCL_{[\aleph]}$, and if any value falls outside of these limits, then the process is declared as out-of-control (OOC); otherwise, it is assumed in-control (IC) point. For a given sampling scheme, the limits, as mentioned above, depend on the choice of n. Therefore, to obtain the

TABLE 1 Control chart constants and probability limits for the $CV_{[NRSS]}$ chart at different levels of n and ARL_0 choices

		$ARL_0 = 100$		$ARL_0 = 200$		$ARL_0 = 370$		$ARL_0 = 500$	
n	k_2	LCL	UCL	LCL	UCL	LCL	UCL	LCL	UCL
3	0.9525	0.3099	1.841	0.2719	1.9341	0.2423	2.0123	0.2293	2.0505
4	0.8861	0.4163	1.4734	0.3836	1.5328	0.3575	1.5826	0.3454	1.6066
5	0.9785	0.5844	1.4426	0.5537	1.489	0.5298	1.5279	0.5181	1.5471
6	0.9457	0.6252	1.3103	0.5994	1.3458	0.5788	1.376	0.5691	1.3904
7	0.9852	0.7057	1.2977	0.6829	1.3277	0.6643	1.3532	0.6552	1.3658
8	0.9662	0.7264	1.2294	0.7065	1.2546	0.6898	1.2758	0.6822	1.2858
9	0.9884	0.7733	1.2225	0.755	1.2445	0.7399	1.2633	0.7329	1.2726
10	0.9761	0.7849	1.1818	0.7686	1.2015	0.7553	1.2173	0.7491	1.2248
11	0.9903	0.8153	1.1774	0.8004	1.1951	0.7877	1.2096	0.782	1.2166
12	0.9817	0.8226	1.1498	0.809	1.1655	0.7976	1.1785	0.7922	1.1848
13	0.9916	0.8441	1.1471	0.8313	1.1615	0.8209	1.1736	0.8162	1.1792
14	0.9853	0.8494	1.1279	0.8378	1.1412	0.8281	1.1519	0.8235	1.1572
15	0.9926	0.8655	1.1257	0.8544	1.1381	0.8452	1.1484	0.8409	1.1531

constant $k_{2[\aleph]}$ and the quantile points of $L_{i[\aleph]}$ (i.e., $LPL_{[\aleph]} = L_{i[\aleph]_{(\alpha/2)}}$, $UPL_{[\aleph]} = L_{i[\aleph]_{(1-\alpha/2)}}$), the following procedure is adopted.

i. Generate 100,000 random samples of size n^2 from the bivariate normal distribution having mean vector μ and covariance matrix Σ, where

$$\mu = (\mu_X, \mu_Z)$$

$$\Sigma = \begin{pmatrix} \frac{(\mu_X\gamma)^2}{n} & \rho\frac{\mu_X\mu_Z\gamma^2}{n} \\ \rho\frac{\mu_X\mu_Z\gamma^2}{n} & \frac{(\mu_Z\gamma)^2}{n} \end{pmatrix}.$$

ii. Obtain 100,000 ranked samples of size n using above-mentioned ranked set schemes.
iii. Calculate sample means $\bar{X}_{i[\aleph]}$ and the standard deviations $S_{i[\aleph]}$, where $i = 1, 2, \ldots, 100,000$.
iv. Based on the $\bar{X}_{i[\aleph]}$ and $S_{i[\aleph]}$, obtain CV estimates ($W_{i[\aleph]}$) by using (2). Further, the $L_{i[\aleph]} = W_{i[\aleph]}/\gamma$ can be estimated based on $W_{i[\aleph]}$ and γ.
v. The mean of $L_{i[\aleph]}$ array is considered as $k_{2[\aleph]}$ value. Similarly, $LPL_{[\aleph]}$ and $UPL_{[\aleph]}$ were estimated as the $(\alpha/2)^{th}$ and $(1-\alpha/2)^{th}$ quantile of $L_{i[\aleph]}$ array.

By using the above-mentioned procedure, values of $k_{2[\text{NRSS}]}$, $LPL_{[NRSS]}$, and $UPL_{[NRSS]}$ were found and are reported in Table 1 with respect to different choices of n and fixed IC average run length equals 100, 200, 370, and 500. Similarly, the values of $k_{2[\aleph]}$, $LPL_{[\aleph]}$, and $UPL_{[\aleph]}$ for $\aleph = SRS, RSS, MRSS$, and $ERSS$ can be seen from Abbasi et al.[50]

3 | PERFORMANCE EVALUATIONS

This section consists of a discussion on performance measures, which are used to evaluate the stated proposal and comparative study. Moreover, the design of the simulated study is also reported in this section.

3.1 | Performance measures

The average run-length (ARL) is the most important measure, used to describe the performance of a control chart. The ARL is defined as the average number of plotting points until a point falls outside the limits (cf. Mahmood and Xie[59]).

Generally, the *ARL* measure is classified into two categories: IC *ARL* (ARL_0) and OUC (ARL_1). When the process is assumed under stable conditions or based on IC parameters, then the *ARL* measure is known by ARL_0 otherwise, the *ARL* measure is termed as ARL_1. A control chart is declared as the best chart among the competing charts, if for a fixed ARL_0, it has a minimum ARL_1 for detecting shifts in process parameters (CV in this case). Furthermore, due to the skewed nature of *ARL* measure, few researchers prefer to evaluate the performance using the median run-length (*MDRL*) and standard deviation of the run-length (*SDRL*). The *MDRL* provides a robust estimate of the run-length of a chart, while *SDRL* is used to show the variation in run-length values. All three measures (*ARL*, *MDRL*, and *SDRL*) are used for performance evaluation of the proposed $CV_{[NRSS]}$ chart. Further, its performance is compared with the CV charts (i.e., $CV_{[SRS]}$, $CV_{[RSS]}$, $CV_{[MRSS]}$, and $CV_{[ERSS]}$) based on SRS, RSS, MRSS, and ERSS schemes.

3.2 | Design of simulation study

To evaluate the performance of the proposed $CV_{[NRSS]}$ chart and for the comparative analysis, a comprehensive simulation study is designed, as described below:

i. Generate a random sample of size n^2 from the bivariate normal distribution with $\mu = (\mu_X, \mu_Z)$ and $\Sigma = \begin{pmatrix} \frac{(\mu_X\gamma_1)^2}{n} & \rho\frac{\mu_X\mu_Z{\gamma_1}^2}{n} \\ \rho\frac{\mu_X\mu_Z{\gamma_1}^2}{n} & \frac{(\mu_Z\gamma_1)^2}{n} \end{pmatrix}$, where γ_1 is equals to $\gamma(1+\delta)$. The process is considered as IC when $\delta = 0$ and when $\delta > 0$, the process is assumed to be OOC.
ii. Obtain ranked set sample of size n using above-mentioned ranked set schemes.
iii. Based on the ranked set sample of size n, compute the $W_{1[\aleph]}$ using (2) and plot it against the control limits based on the choice of n provided in Table 1.
iv. If $W_{1[\aleph]}$ falls in the limits, then repeat steps (i-iii) until $W_{i[\aleph]}$ falls outside of the limits. Note the i as the first run-length value.
v. Repeat steps i-iv, a large number of times say 100,000 times and record the run-length values.

Further, the performance measures, such as *ARL*, *MDRL*, and *SDRL*, were computed as the mean, median, and standard deviation of these 100,000 run-length values, respectively.

The performance of the $CV_{[NRSS]}$ control chart is evaluated based on the different choices of sample size ($n = 3, 5, 7$, and 10) and several choices of ${ARL_0}'s$, such as 100, 200, 370, and 500. Further, the shift size δ is considered as $0.05, 0.1, 0.15, 0.2, 0.25, 0.3, 0.4, 0.5, 1$, and 2. It is noted that the stated study is designed under the perfect ranking conditions ($\rho = 1$) as well as under the imperfect ranking situation ($\rho = 0.25, 0.5, 0.75$, and 0.9).

4 | RESULTS AND DISCUSSIONS

In this section, first, we will evaluate the performance of the proposed $CV_{[NRSS]}$ chart in terms of *ARL*, *MDRL*, and *SDRL* with respect to different choices of ARL_0, such as 100, 200, 370, and 500 in Tables 2–5. Moreover, the effect of the perfect and imperfect ranking situations on the performance of the $CV_{[NRSS]}$ chart is reported in Table 6. Finally, the comparison of $CV_{[NRSS]}$ chart with the $CV_{[SRS]}$, $CV_{[RSS]}$, $CV_{[MRSS]}$, and $CV_{[ERSS]}$ charts is presented in Figures 1 and 2. The finding depicts that:

- The detection ability of the $CV_{[NRSS]}$ chart increases with the increase of shifts in the mean. For example, on the fixed $ARL_0 = 100$ and sample size $n = 7$, the ARL_1 for $CV_{[NRSS]}$ chart is reported 51.14 with $\delta = 0.05$, while the ARL_1 decreases and reported 3.19 against $\delta = 0.25$ (Table 2). Similar performance behavior is revealed under all choices of sample size and ARL_0 (Table 2–6).
- The power of detection for the $CV_{[NRSS]}$ chart increases with an increase in the level of sample size n. For instance, on the fixed $ARL_0 = 500$ and $\delta = 0.15$, the ARL_1 for $CV_{[NRSS]}$ chart is 119.76 with choice of sample size $n = 3$, while the ARL_1 decreases and reported 2.39 against $n = 15$ (Table 5). A similar pattern of detection ability revealed under all choices of δ and ARL_0 (Table 2–6).

TABLE 2 Run length characteristics of $CV_{[NRSS]}$ chart at different levels of n when $ARL_0 = 100$

n	δ	0.00	0.05	0.10	0.15	0.20	0.25	0.30	0.40	0.50	1.00	2.00
3	ARL	99.25	74.73	52.19	35.64	24.64	17.95	13.37	8.15	5.53	1.96	1.15
	MDRL	69	51	35	25	17	13	9	6	4	1	1
	SDRL	99.56	75.61	53.08	35.82	24.41	17.47	13.01	7.57	4.96	1.35	0.41
5	ARL	101.12	63.36	32.73	17.69	10.36	6.75	4.73	2.71	1.89	1.06	1
	MDRL	70	44	23	13	7	5	3	2	1	1	1
	SDRL	99.9	62.53	32.55	17.16	9.79	6.17	4.15	2.13	1.29	0.25	0.02
7	ARL	100.44	51.14	20.23	9.31	5.03	3.19	2.25	1.46	1.17	1	1
	MDRL	70	36	14	7	4	2	2	1	1	1	1
	SDRL	101.08	50.67	19.98	8.76	4.57	2.68	1.67	0.8	0.44	0.03	0
10	ARL	98.87	33.46	9.85	4.04	2.23	1.54	1.24	1.04	1	1	1
	MDRL	68	24	7	3	2	1	1	1	1	1	1
	SDRL	97.99	32.62	9.56	3.52	1.63	0.92	0.55	0.21	0.07	0	0
15	ARL	98.69	16.68	3.72	1.66	1.17	1.03	1	1	1	1	1
	MDRL	69	12	3	1	1	1	1	1	1	1	1
	SDRL	99.36	16.07	3.18	1.04	0.44	0.18	0.07	0	0	0	0

TABLE 3 Run length characteristics of $CV_{[NRSS]}$ chart at different levels of n when $ARL_0 = 200$

n	δ	0.00	0.05	0.10	0.15	0.20	0.25	0.30	0.40	0.50	1.00	2.00
3	ARL	198.92	143.36	92.65	59.42	39.54	27.05	19.51	11.34	7.25	2.21	1.19
	MDRL	137	99	64	40	27	19	14	8	5	2	1
	SDRL	197.89	144.5	93.27	59.94	39.39	26.78	19.17	10.83	6.64	1.62	0.47
5	ARL	200.91	118.45	55.56	27.81	15.47	9.46	6.28	3.37	2.2	1.08	1
	MDRL	140	81	39	20	11	7	5	2	2	1	1
	SDRL	199.36	119.34	54.65	27.36	14.94	8.95	5.71	2.79	1.6	0.3	0.02
7	ARL	199.38	90.56	32.16	13.63	6.86	4.04	2.73	1.61	1.24	1	1
	MDRL	138	63	22	10	5	3	2	1	1	1	1
	SDRL	195.69	91.1	32.2	13.29	6.36	3.55	2.16	0.97	0.53	0.04	0
10	ARL	199.7	57.28	14.75	5.42	2.73	1.75	1.35	1.06	1.01	1	1
	MDRL	139	40	10	4	2	1	1	1	1	1	1
	SDRL	200.31	56.57	14.4	4.94	2.18	1.15	0.68	0.26	0.1	0	0
15	ARL	199.45	26.69	5.02	1.91	1.25	1.05	1.01	1	1	1	1
	MDRL	140	19	4	1	1	1	1	1	1	1	1
	SDRL	196.48	26.05	4.5	1.33	0.54	0.23	0.1	0	0	0	0

- The correlation factor ρ often selected to determine the ranking strategy used for the generation of NRSS samples. When $\rho < 1$, a ranking strategy is known by imperfect ranking, and it is assumed perfect ranking when $\rho = 1$. The shift detection ability of the $CV_{[NRSS]}$ chart increases with an increase in the level of ρ. For example, on the fixed $ARL_0 = 370, n = 5$ and $\delta = 0.25$, the ARL_1 of $CV_{[NRSS]}$ chart is 43.77 when $\rho = 0.25$, while the ARL_1 decreases and noted 12.78 against $\rho = 1$ (Table 6). Hence, it is concluded that the $CV_{[NRSS]}$ chart showed superior performance under perfect ranking.

Abbasi et al[50] proposed Shewhart-type CV control charts based on RSS, MRSS, and ERSS strategies. Their respective charts are referred as $CV_{[RSS]}$, $CV_{[MRSS]}$, and $CV_{[ERSS]}$ charts. They have compared these charts with the conventional $CV_{[SRS]}$ chart and concluded that the $CV_{[ERSS]}$ chart has better detection ability as compared to all other charts. In this study, we are comparing the proposed $CV_{[NRSS]}$ chart with the $CV_{[SRS]}$, $CV_{[RSS]}$, $CV_{[MRSS]}$, and $CV_{[ERSS]}$ charts. The $log(ARL)$ for each chart, with respect to several levels of shifts in process CV, is plotted in Figures 1 and 2. In this comparative study, perfect sampling mechanism (i.e., $\rho = 1$) is considered with the fixed $ARL_0 = 370$.

TABLE 4 Run length characteristics of $CV_{[NRSS]}$ chart at different levels of n when $ARL_0 = 370$

n	δ	0.00	0.05	0.10	0.15	0.20	0.25	0.30	0.40	0.50	1.00	2.00
3	ARL	370.72	253.64	156.35	94.83	59.67	39.71	27.39	14.99	9.31	2.46	1.23
	MDRL	257	175	107	65	41	27	19	10	7	2	1
	SDRL	369.24	251.95	156.27	95.21	59.82	39.72	27.17	14.55	8.77	1.89	0.52
5	ARL	367.75	203.7	89.67	42.09	21.85	12.78	8.2	4.1	2.52	1.11	1
	MDRL	259	143	63	30	16	9	6	3	2	1	1
	SDRL	362.07	201	88.42	41.47	21.43	12.19	7.63	3.54	1.94	0.34	0.03
7	ARL	370.39	153.12	49.72	19.48	9.2	5.11	3.27	1.8	1.31	1	1
	MDRL	254	106	34	14	7	4	2	1	1	1	1
	SDRL	367.48	153.82	49.64	19.21	8.67	4.67	2.78	1.19	0.63	0.05	0
10	ARL	370.07	92.63	20.96	7.1	3.33	1.98	1.45	1.09	1.01	1	1
	MDRL	255.5	64	15	5	2	1	1	1	1	1	1
	SDRL	367.92	92.85	20.34	6.78	2.77	1.39	0.8	0.3	0.12	0	0
15	ARL	371.03	40.5	6.57	2.22	1.33	1.07	1.01	1	1	1	1
	MDRL	261	28	5	2	1	1	1	1	1	1	1
	SDRL	363.29	39.73	6.07	1.67	0.66	0.28	0.12	0.01	0	0	0

TABLE 5 Run length characteristics of $CV_{[NRSS]}$ chart at different levels of n when $ARL_0 = 500$

n	δ	0.00	0.05	0.10	0.15	0.20	0.25	0.30	0.40	0.50	1.00	2.00
3	ARL	504.08	338.86	202.18	119.76	73.2	48.03	32.92	17.41	10.46	2.61	1.24
	MDRL	352	238	139	83	50	33	22	12	7	2	1
	SDRL	499.62	337.5	202.88	119.48	73.75	48.27	33.07	16.95	9.91	2.03	0.54
5	ARL	499.59	271.07	115.23	51.33	26.24	14.94	9.34	4.57	2.73	1.12	1
	MDRL	348	188	79	36	19	11	7	3	2	1	1
	SDRL	500.58	269.38	115.82	50.39	25.71	14.43	8.84	4.02	2.15	0.36	0.03
7	ARL	499.32	198.75	61.52	23.29	10.7	5.78	3.58	1.9	1.36	1	1
	MDRL	349	139	43	16	8	4	3	1	1	1	1
	SDRL	496.99	194.77	60.92	23.2	10.22	5.29	3.12	1.3	0.69	0.06	0
10	ARL	502.36	116.1	25.19	8.12	3.64	2.11	1.51	1.1	1.02	1	1
	MDRL	356	79	18	6	3	2	1	1	1	1	1
	SDRL	495.31	117.66	24.6	7.89	3.1	1.51	0.88	0.33	0.13	0	0
15	ARL	503.04	49.36	7.47	2.39	1.38	1.09	1.02	1	1	1	1
	MDRL	350	34	5	2	1	1	1	1	1	1	1
	SDRL	496.3	48.49	6.99	1.86	0.72	0.31	0.13	0.01	0	0	0

- From Figures 1 and 2, it is clearly observed that the $CV_{[NRSS]}$ chart has the lowest ARL curves as compared to the $CV_{[SRS]}$, $CV_{[RSS]}$, $CV_{[MRSS]}$, and $CV_{[ERSS]}$ charts, considering samples sizes n = 5 and 10, respectively.
- Hence, it is concluded that the $CV_{[NRSS]}$ chart is the best performing chart among all other competing CV charts, to detect a change in the process CV.

5 | AN ILLUSTRATIVE EXAMPLE

For the illustration of $CV_{[\aleph]}$ charts, we have considered nonisothermal Continuous Stirred Tank Chemical Reactor (CSTR) dataset obtained from Yoon and MacGregor.[60] Usually, a nonisothermal CSTR is used to illustrate the fault isolation. The process plotted in Figure 3 consists of a feed stream, a product stream, and a cooling water flow to the coils. The feed stream is a merged stream of the reactant A and the solvent. The first-order reaction ($A \rightarrow B$) was considered and reactor system involves heat transfer and heat of reaction. Further, it was also assumed that the tank is well mixed, and the physical

TABLE 6 Run length characteristics of $CV_{[NRSS]}$ chart with respect to perfect and imperfect ranking when $n = 5$ and $ARL_0 = 370$

ρ	δ	0.00	0.05	0.10	0.15	0.20	0.25	0.30	0.40	0.50	1.00	2.00
0.25	ARL	370.29	250.63	158.12	100.59	65.12	43.77	30.96	17.07	10.64	2.96	1.39
	MDRL	256	174	110	70	45	30	22	12	8	2	1
	SDRL	367.21	248.24	158.69	100.13	64.56	43.37	30.26	16.49	10.17	2.41	0.76
0.5	ARL	368.96	249.74	156.07	95.34	60.24	40.59	28.69	15.58	9.86	2.72	1.34
	MDRL	254	174	109	66	42	28	20	11	7	2	1
	SDRL	368.4	249.11	155.11	95.58	59.84	39.96	27.99	15.1	9.3	2.18	0.68
0.75	ARL	371.72	237.76	137.93	78.85	48.86	31.73	21.78	11.85	7.44	2.17	1.21
	MDRL	262	167	96	55	34	22	15	9	5	2	1
	SDRL	366.77	235.14	134.66	79.03	48.79	31.09	21.56	11.28	6.81	1.62	0.5
0.9	ARL	370.08	219.6	115.32	61.99	35.63	21.98	14.58	7.73	4.79	1.59	1.07
	MDRL	256	154	79	42	25	16	10	5	3.5	1	1
	SDRL	368.29	219.46	115.2	62.23	35.26	21.15	13.97	7.24	4.27	0.97	0.29
1	ARL	367.75	203.7	89.67	42.09	21.85	12.78	8.2	4.1	2.52	1.11	1
	MDRL	259	143	63	30	16	9	6	3	2	1	1
	SDRL	362.07	201	88.42	41.47	21.43	12.19	7.63	3.54	1.94	0.34	0.03

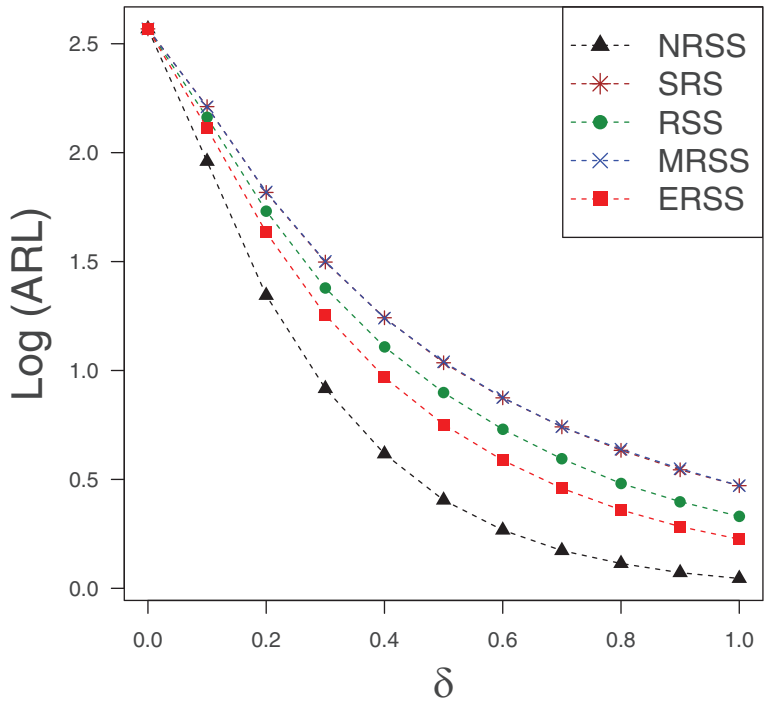

FIGURE 1 Comparison between $CV_{[\aleph]}$ charts at fixed sample size $n = 5$ and $ARL_0 = 370$

properties are constant. In total, nine variables have been collected on sampling interval of a half-minute to construct the detection model, such as flow rate of reactant A (m^3/min), flow rate of cooling water (m^3/min), outlet concentration of the product (kmole/m^3), outlet temperature (K), inlet concentration of solvent flow (kmole/m^3), inlet concentration of solute A (kmole/m^3), inlet temperature (K), flow rate of the solvent (m^3/min), and cooling water temperature (K).

Among all fault detection indicators, outlet temperature is an important variable that shows the variation in the temperature of the whole system. Therefore, we have considered outlet temperature as a study variable and obtained 40 sets each of size 5 (i.e., $n = 5$) using the different sampling schemes, such as RSS, MRSS, ERSS, and NRSS. Further, for checking the consistency of $CV_{[\aleph]}$ statistics, $\bar{X}_{i[\aleph]}; i = 1, 2, \ldots, 40$, are plotted against the $\hat{\gamma}^2_{i[\aleph]}$ in Figure 4, following Kang et al[10] and Abbasi et al.[50] The scatter plots of $\bar{X}_{[\aleph]}$ and $\hat{\gamma}^2_{[\aleph]}$ showed that the $CV_{[\aleph]}$ statistics are constant against the $\bar{X}_{[\aleph]}$. Furthermore, a hypothesis test is also implemented using the regression model to check the constant $CV_{[\aleph]}$ statistic against $\bar{X}_{[\aleph]}$.

FIGURE 2 Comparison between $CV_{[\aleph]}$ charts at fixed sample size $n = 10$ and $ARL_0 = 370$

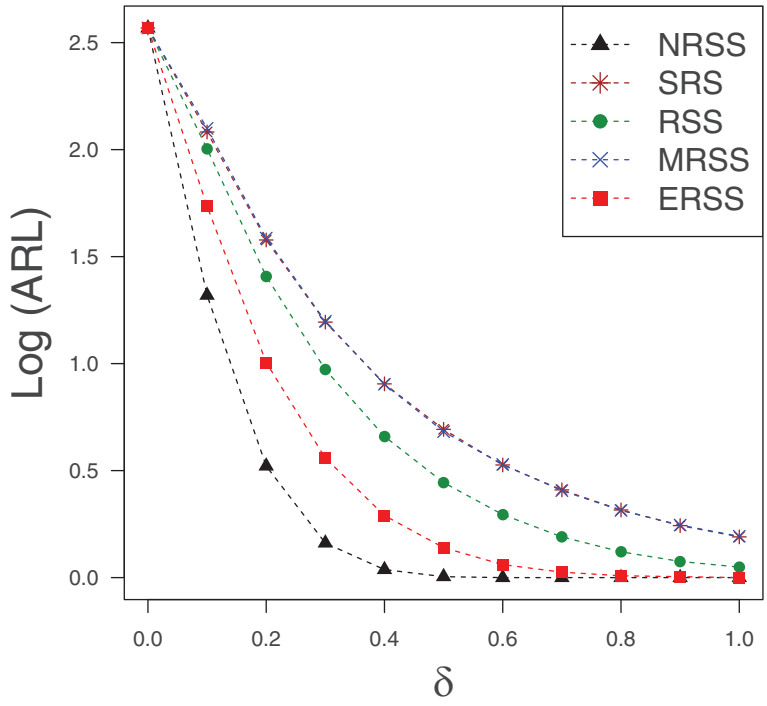

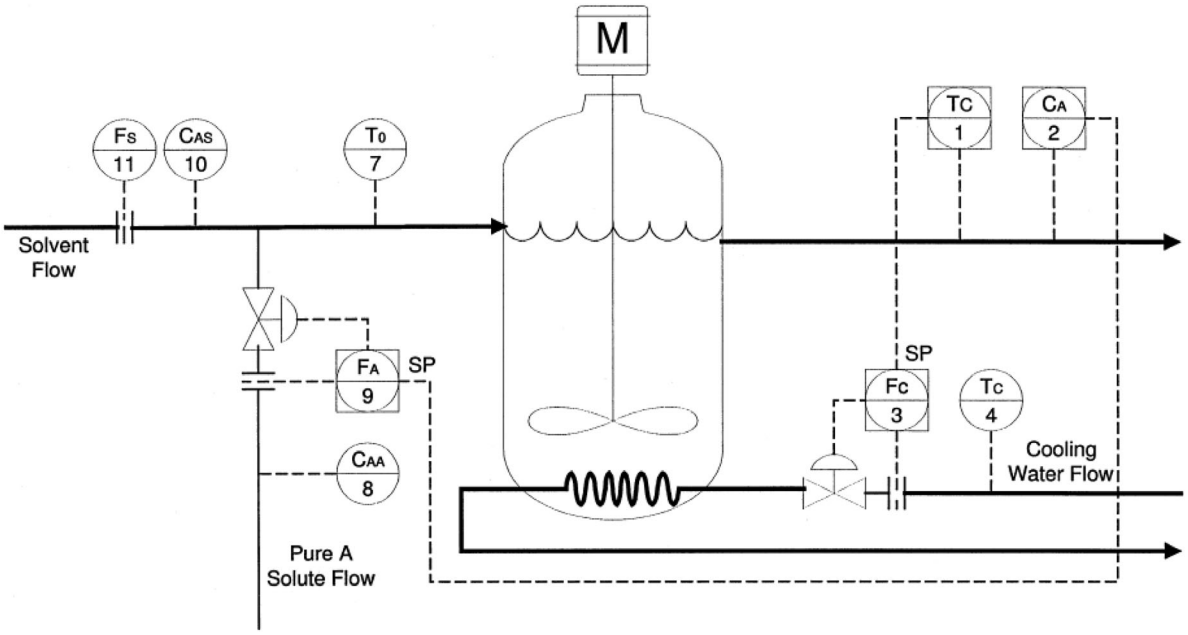

FIGURE 3 Diagram of the CSTR system (Yoon and MacGregor[60])

Under the null hypothesis, it is assumed that the $CV_{[\aleph]}$ statistics are constant against $\bar{X}_{[\aleph]}$, while nonconstant behavior is considered under the alternative hypothesis. The regression results with respect to sampling schemes are reported in Table 7, where all P-values are higher than the level of significance (i.e., $\alpha = 0.05$), which supports the null hypothesis that the $CV_{[\aleph]}$ statistics are constant against $\bar{X}_{[\aleph]}$. From Figure 4, it is also revealed that there is no apparent correlation structure between $\bar{X}_{[\aleph]}$ and $\hat{\gamma}^2_{[\aleph]}$. Hence, based on these two findings, it is justified to use $CV_{[\aleph]}$ charts to detect a change in outlet temperature.

Based on all sets, the estimated IC $\hat{\gamma}_{[\aleph]}$ were obtained, which are reported in Table 8. Further, at fixed $ARL_0 = 200$ and by using $\hat{\gamma}_{[\aleph]}$, the control limits (i.e., $LCL_{[\aleph]}$ and $UCL_{[\aleph]}$) were obtained, which are also given in Table 8. Furthermore, the $CV_{[\aleph]}$ statistics for each set are presented in Table 8. To illustrate the shifted behavior, we considered the first 34 samples as

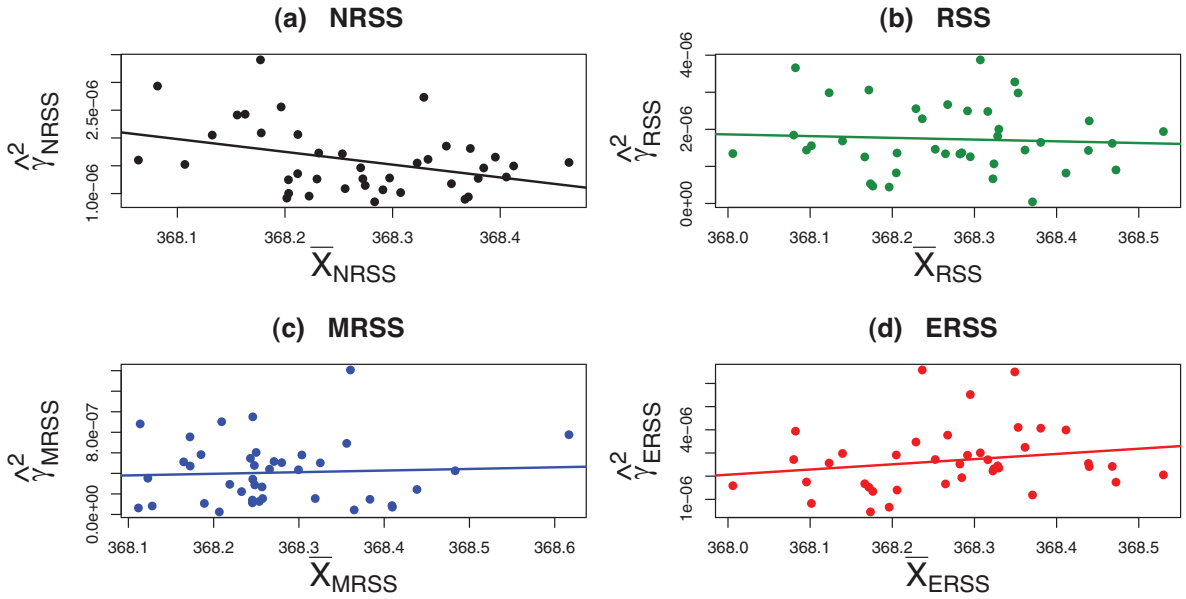

FIGURE 4 Scatter plot of $\bar{X}_{[\aleph]}$ and $\hat{\gamma}^2_{[\aleph]}$ for the CSTR data

TABLE 7 Regression test results for CSTR example

	Source of variation	Degrees of freedom	Sum of squares	Mean square	*F*-value	*P*-value
$CV_{[NRSS]}$	Model	1	2.06E-12	2.07E-12	3.330	.0759
	Error	38	2.36E-11	6.21E-13		
	Total	39	2.56481E-11			
$CV_{[RSS]}$	Model	1	1.87E-07	1.87E-07	1.420	.2408
	Error	38	5.00E-06	1.31E-07		
	Total	39	5.18E-06			
$CV_{[MRSS]}$	Model	1	4.89E-10	4.89E-10	0.007	.9326
	Error	38	2.56E-06	6.74E-08		
	Total	39	2.56E-06			
$CV_{[ERSS]}$	Model	1	1.20E-08	1.20E-08	0.081	.7774
	Error	38	5.64E-06	1.48E-07		
	Total	39	5.65E-06			

IC, while in the last 6 samples, a shift of size $\delta = 2$ is introduced. The $CV_{[\aleph]}$ statistics are reported in Table 9 and are plotted against their respected limits (i.e., $LCL_{[\aleph]}$ and $UCL_{[\aleph]}$) in Figure 5. The findings reveal that all signals are detected through $CV_{[NRSS]}$ chart, while $CV_{[RSS]}$ chart detects two signals, $CV_{[MRSS]}$ chart detects only one signal, and $CV_{[ERSS]}$ chart has detected three signals. This shows the superiority of using $CV_{[RSS]}$ chart, as compared to other competing charts. These findings support the simulation results where the $CV_{[NRSS]}$ chart was declared superior as compared to all other charts.

TABLE 8 CV estimates and control limits based on different sampling schemes for CSTR data

	NRSS	*RSS*	*MRSS*	*ERSS*
$\hat{\gamma}_{[\aleph]}$	0.001217	0.001326	0.000674	0.001599
$LCL_{[\aleph]}$	0.000661	0.000328	0.000114	0.000534
$UCL_{[\aleph]}$	0.001891	0.002743	0.001508	0.003140

TABLE 9 Plotting statistics for the $CV_{[\aleph]}$ charts based on different sampling schemes

Sample No.	*RSS*	*MRSS*	*ERSS*	*NRSS*	Sample No.	*RSS*	*MRSS*	*ERSS*	*NRSS*
1	0.00162	0.00117	0.00054	0.001390178	21	0.00122	0.00130	0.00059	0.00173
2	0.00105	0.00128	0.00071	0.002017729	22	0.00134	0.00117	0.00074	0.00118
3	0.00113	0.00160	0.00026	0.001863066	23	0.00129	0.00091	0.00087	0.00171
4	0.00161	0.00163	0.00025	0.001941597	24	0.00087	0.00125	0.00038	0.00091
5	0.00084	0.00120	0.00095	0.00132362	25	0.00067	0.00103	0.00021	0.00152
6	0.00091	0.00173	0.00076	0.001602703	26	0.00140	0.00191	0.00072	0.00199
7	0.00071	0.00151	0.00098	0.002565132	27	0.00081	0.00173	0.00065	0.00203
8	0.00052	0.00121	0.00078	0.001649373	28	0.00103	0.00082	0.00083	0.00149
9	0.00112	0.00095	0.00029	0.001320259	29	0.00132	0.00112	0.00076	0.00235
10	0.00092	0.00197	0.00071	0.001735428	30	0.00063	0.00116	0.00069	0.00126
11	0.00146	0.00120	0.00052	0.001800674	31	0.00104	0.00120	0.00049	0.00160
12	0.00048	0.00112	0.00094	0.001293585	32	0.00139	0.00158	0.00119	0.00165
13	0.00178	0.00116	0.00059	0.001588842	33	0.00143	0.00127	0.00039	0.00156
14	0.00080	0.00175	0.00016	0.001233233	34	0.00143	0.00136	0.00069	0.00165
15	0.00049	0.00069	0.00036	0.001157922	35	0.00361	0.00269	0.00139	0.00322
16	0.00106	0.00116	0.00033	0.001290585	36	0.00329	0.00265	0.00185	0.00301
17	0.00161	0.00158	0.00047	0.001705043	37	0.00345	0.00344	0.00061	0.00535
18	0.00175	0.00091	0.00066	0.001999052	38	0.00167	0.00139	0.00071	0.00143
19	0.00063	0.00067	0.00054	0.000810906	39	0.00142	0.00041	0.00083	0.00229
20	0.00108	0.00135	0.00072	0.001564421	40	0.00371	0.00284	0.00080	0.00326

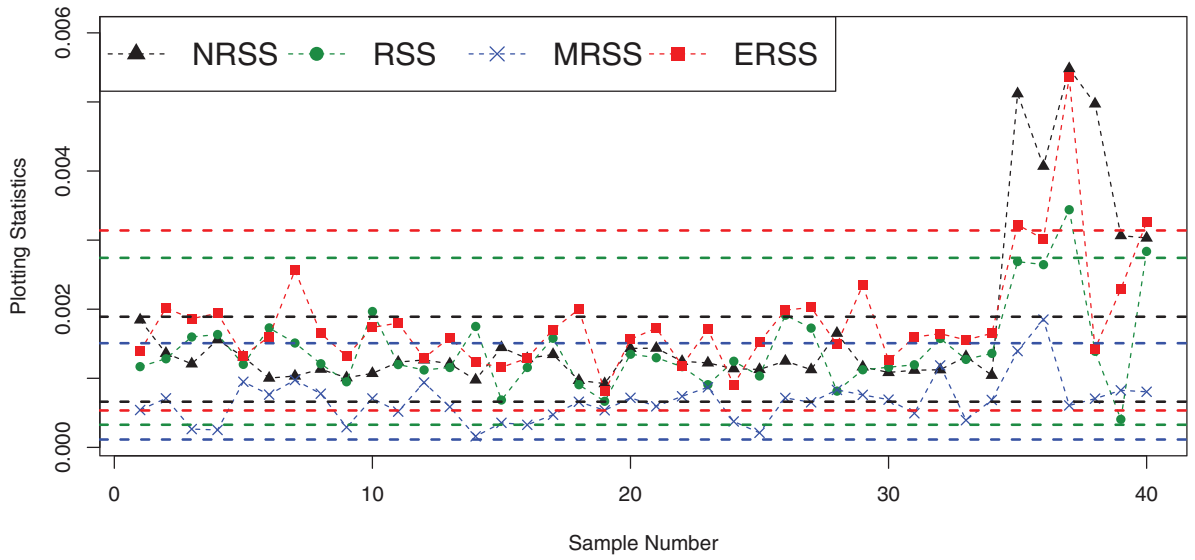

FIGURE 5 Plot of $CV_{[\aleph]}$ charts for the CSTR data

6 | CONCLUSIONS AND RECOMMENDATIONS

The CV chart is often used to monitor the relative variability in the process. In this study, we have proposed a Shewhart-based CV chart, considering a newly introduced NRSS, which is referred as the $CV_{[\text{NRSS}]}$ chart. An extensive simulation study is designed to evaluate the performance of $CV_{[\text{NRSS}]}$ chart in terms of *ARL*, *MDRL*, and *SDRL* measures. The findings depict that the performance of the $CV_{[\text{NRSS}]}$ chart improves with an increase of sample size n. The $CV_{[\text{NRSS}]}$

has highest detection ability under the perfect RSS mechanism. Moreover, the comparison of $CV_{[NRSS]}$ chart with the existing competitive charts (such as $CV_{[SRS]}$, $CV_{[RSS]}$, $CV_{[MRSS]}$, and charts) revealed the superiority of the $CV_{[NRSS]}$ chart, in terms of detecting shifts in process CV. The implementation of the CV charts on the CSTR dataset also indicated the superiority of $CV_{[NRSS]}$ chart, compared to other charts.

The study can be extended for efficient detection of shifts in multivariate CV or by considering the auxiliary-based estimates of process CV, mentioned in Abbasi.[61] Moreover, to obtain further improvements for the detection of small or moderate shifts, EWMA and CUSUM-type structures can be the possible extensions to the $CV_{[NRSS]}$ chart.

ORCID

Tahir Mahmood https://orcid.org/0000-0002-8748-5949
Saddam Akber Abbasi https://orcid.org/0000-0003-1843-8863

REFERENCES

1. Montgomery DC. *Introduction to Statistical Quality Control*. 6th ed. New York: John Wiley & Sons; 2009.
2. Schoonhoven M, Nazir HZ, Riaz M, Does RJ. Robust location estimators for the X-bar control chart. *J Qual Technol*. 2011;43:363-379.
3. Nazir HZ, Schoonhoven M, Riaz M, Does RJ. Quality quandaries: a stepwise approach for setting up a robust Shewhart location control chart. *Qual Eng*. 2014;26:246-252.
4. Abbasi SA, Miller A. On proper choice of variability control chart for normal and non-normal processes. *Qual Reliab Eng Int*. 2012;28:279-296.
5. Ali A, Mahmood T, Nazir HZ, et al. Control charts for process dispersion parameter under contaminated normal environments. *Qual Reliab Eng Int*. 2016;32:2481-2490.
6. Abbas N, Riaz M, Mahmood T. An improved S^2 control chart for cost and efficiency optimization. *IEEE Access*. 2017;5:19486-19493.
7. Mahmood T, Nazir HZ, Abbas N, Riaz M, Ali A. Performance evaluation of joint monitoring control charts. *Sci Iran*. 2017;24:2152-2163.
8. Zafar RF, Mahmood T, Abbas N, Riaz M, Hussain Z. A progressive approach to joint monitoring of process parameters. *Comput Ind Eng*. 2018;115:253-268.
9. Sanusi RA, Mukherjee A, Xie M. A comparative study of some EWMA schemes for simultaneous monitoring of mean and variance of a Gaussian process. *Comput Ind Eng*. 2019;135:426-439.
10. Kang CW, Lee MS, Seong YJ, Hawkins DM. A control chart for the coefficient of variation. *J Qual Technol*. 2007;39:151-158.
11. Connett JE, Lee WW. Estimation of the coefficient of variation from laboratory analysis of split specimens for quality control in clinical trials. *Control Clin Trials*. 1990;11:24-36.
12. Hong E-P, Kang C-W, Baek J-W, Kang H-W. Development of CV control chart using EWMA technique. *J Soc Korea Ind Syst Eng*. 2008;31:114-120.
13. Menzefricke U. Control charts for the variance and coefficient of variation based on their predictive distribution. *Commun Statist—Theory Methods*. 2010;39:2930-2941.
14. Castagliola P, Celano G, Psarakis S. Monitoring the coefficient of variation using EWMA charts. *J Qual Technol*. 2011;43:249-265.
15. Zhang J, Li Z, Chen B, Wang Z. A new exponentially weighted moving average control chart for monitoring the coefficient of variation. *Comput Ind Eng*. 2014;78:205-212.
16. Hong EP, Kang HW, Kang CW. DEWMA control chart for the coefficient of variation. *Adv Mater Res*. 2011;201-203:1682-1688.
17. Calzada ME, Scariano SM. A synthetic control chart for the coefficient of variation. *J Statist Comput Simul*. 2013;83:853-867.
18. Castagliola P, Achouri A, Taleb H, Celano G, Psarakis S. Monitoring the coefficient of variation using control charts with run rules. *Qual Technol Quant Manage*. 2013;10:75-94.
19. Castagliola P, Amdouni A, Taleb H, Celano G. One-sided Shewhart-type charts for monitoring the coefficient of variation in short production runs. *Qual Technol Quant Manage*. 2015;12:53-67.
20. Yeong WC, Chuah ME, Teoh WL, Khoo MBC, Lim SL. The economic and economic-statistical designs of the coefficient of variation chart. *Acad J Sci*. 2015;4:57-72.
21. Tran PH, Tran KP. The efficiency of CUSUM schemes for monitoring the coefficient of variation. *Appl Stochastic Mod Bus Ind*. 2016;32:870-881.
22. You HW, Khoo MB, Castagliola P, Haq A. Monitoring the coefficient of variation using the side sensitive group runs chart. *Qual Reliab Eng Int*. 2016;32:1913-1927.
23. Castagliola P, Achouri A, Taleb H, Celano G, Psarakis S. Monitoring the coefficient of variation using a variable sampling interval control chart. *Qual Reliab Eng Int*. 2013;29:1135-1149.
24. Castagliola P, Achouri A, Taleb H, Celano G, Psarakis S. Monitoring the coefficient of variation using a variable sample size control chart. *Int J Adv Manufac Technol*. 2015;80:1561-1576.
25. Amdouni A, Castagliola P, Taleb H, Celano G. Monitoring the coefficient of variation using a variable sample size control chart in short production runs. *Int J Adv Manufac Technol*. 2015;81:1-14.

26. Amdouni A, Castagliola P, Taleb H, Celano G. A variable sampling interval Shewhart control chart for monitoring the coefficient of variation in short production runs. *Int J Prod Res*. 2017;55:5521-5536.
27. Khaw KW, Khoo MB, Yeong WC, Wu Z. Monitoring the coefficient of variation using a variable sample size and sampling interval control chart. *Commun Statist-Simul Comput*. 2017;46:5772-5794.
28. Yeong WC, Khoo MB, Lim SL, Lee MH. A direct procedure for monitoring the coefficient of variation using a variable sample size scheme. *Commun Statist-Simul Comput*. 2017;46:4210-4225.
29. Muhammad ANB, Yeong WC, Chong ZL, Lim SL, Khoo MBC. Monitoring the coefficient of variation using a variable sample size EWMA chart. *Comput Ind Eng*. 2018;126:378-398.
30. Yeong WC, Khoo MBC, Lim SL, Teoh WL. The coefficient of variation chart with measurement error. *Qual Technol Quant Manage*. 2017;14:353-377.
31. Van Zyl R, Van der Merwe A. A Bayesian control chart for a common coefficient of variation. *Commun Statist-Theory Methods*. 2017;46:5795-5811.
32. Teoh WL, Khoo MB, Castagliola P, Yeong WC, Teh SY. Run-sum control charts for monitoring the coefficient of variation. *Eur J Oper Res*. 2017;257:144-158.
33. Yeong WC, Khoo MBC, Teoh WL, Castagliola P. A control chart for the multivariate coefficient of variation. *Qual Reliab Eng Int*. 2016;32:1213-1225.
34. Lim AJ, Khoo MB, Teoh WL, Haq A. Run sum chart for monitoring multivariate coefficient of variation. *Comput Ind Eng*. 2017;109:84-95.
35. Tran KP, Nguyen H, Nguyen QT, Chattinnawat W. One-sided synthetic control charts for monitoring the coefficient of variation with measurement errors. In: *2018 IEEE International Conference on Industrial Engineering and Engineering Management (IEEM)*. IEEE; 2018.
36. Guo B, Wang BX. Control charts for the coefficient of variation. *Statist Papers*. 2018;59:933-955.
37. Khaw KW, Khoo MB, Castagliola P, Rahim M. New adaptive control charts for monitoring the multivariate coefficient of variation. *Comput Ind Eng*. 2018;126:595-610.
38. Dawod AB, Abbasi SA, Al-Momani M. On the performance of coefficient of variation control charts in phase I. *Qual Reliab Eng Int*. 2018;34:1029-1040.
39. Abbasi SA, Adegoke NA. Multivariate coefficient of variation control charts in phase I of SPC. *Int J Adv Manufac Technol*. 2018;99:1903-1916.
40. Yan A-J, Aslam M, Azam M, Jun C-H. Developing a variable repetitive group sampling plan based on the coefficient of variation. *J Ind Prod Eng*. 2017;34:398-405.
41. Yan A, Liu S, Azam M. Designing a multiple state repetitive group sampling plan based on the coefficient of variation. *Commun Statist-Simul Comput*. 2017;46:7154-7165.
42. Ng PS, Khoo MBC, Saha S, Yeong WC. Double sampling control charts for monitoring the coefficient of variation. In: *2018 2nd International Conference on Smart Sensors and Application (ICSSA)*. IEEE; 2018.
43. Teoh WL, Lim J, Khoo MB, Chong ZL, Yeong WC. Optimal designs of EWMA charts for monitoring the coefficient of variation based on median run length and expected median run length. *J Test Eval*. 2018;47:459-479.
44. Zhang J, Li Z, Wang Z. Control chart for monitoring the coefficient of variation with an exponentially weighted moving average procedure. *Qual Reliab Eng Int*. 2018;34:188-202.
45. Du Nguyen H, Nguyen QT, Tran KP, Ho DP. On the performance of VSI Shewhart control chart for monitoring the coefficient of variation in the presence of measurement errors. *Int J Adv Manufac Technol*. 2019;104:211-243.
46. Yeong WC, Lim SL, Khoo MBC, Castagliola P. Monitoring the coefficient of variation using a variable parameters chart. *Qual Eng*. 2018;30:212-235.
47. Chew X, Khoo MBC, Khaw KW, Yeong WC, Chong ZL. A proposed variable parameter control chart for monitoring the multivariate coefficient of variation. *Qual Reliab Eng Int*. 2019;35:2442-2461.
48. Khatun M, Khoo MB, Lee MH, Castagliola P. One-sided control charts for monitoring the multivariate coefficient of variation in short production runs. *Trans Inst Meas Control*. 2019;41:1712-1728.
49. McIntyre G. A method for unbiased selective sampling, using ranked sets. *Aust J Agric Res*. 1952;3:385-390.
50. Abbasi SA, Abbas T, Adegoke NA. Efficient CV control charts based on ranked set sampling. *IEEE Access*. 2019;7:78050-78062.
51. Noor-ul-Amin M, Riaz A. EWMA control chart for coefficient of variation using log-normal transformation under ranked set sampling. *Iran J Sci Technol Trans A Sci*. 2020;44:155-165.
52. Zamanzade E, Al-Omari AI. New ranked set sampling for estimating the population mean and variance. *Hacettepe J Math Statist*. 2016;45:1891-1905.
53. Nawaz T, Raza MA, Han D. A new approach to design efficient univariate control charts to monitor the process mean. *Qual Reliab Eng Int*. 2018;34:1732-1751.
54. Nawaz T, Han D. Monitoring the process location by using new ranked set sampling-based memory control charts. *Qual Technol Quant Manage*. 2020;17:255-284.
55. Abbas T, Mahmood T, Riaz M, Abid M. Improved linear profiling methods under classical and Bayesian setups: an application to chemical gas sensors. *Chemom Intell Lab Syst*. 2020;196:103908.
56. Hussain S, Mahmood T, Riaz M, Nazir HZ. A new approach to design median control charts for location monitoring. *Commun Statist-Simul Comput* 2020. https://doi.org/10.1080/03610918.2020.1716245.
57. Muttlak H. Median ranked set sampling. *J Appl Statist Sci*. 1997;6:245-255.

58. Samawi HM, Ahmed MS, Abu-Dayyeh W. Estimating the population mean using extreme ranked set sampling. *Biometrical J*. 1996;38:577-586.
59. Mahmood T, Xie M. Models and monitoring of zero-inflated processes: the past and current trends. *Qual Reliab Eng Int*. 2019;35:2540-2557.
60. Yoon S, MacGregor JF. Fault diagnosis with multivariate statistical models part I: using steady state fault signatures. *J Process Control*. 2001;11:387-400.
61. Abbasi SA. Efficient charts for monitoring process CV using auxiliary information. *IEEE Access*. 2020;8:46176-46192.

AUTHOR BIOGRAPHIES

Tahir Mahmood got his degree of BS (Hons.) in Statistics with distinction (Gold Medalist) from the Department of Statistics, University of Sargodha, Sargodha, Pakistan. He has received MS (Applied Statistics) degree from Department of Mathematics and Statistics, King Fahd University of Petroleum and Minerals (KFUPM), Dhahran, Saudi Arabia. He received his PhD degree from the Department of Systems Engineering and Engineering Management, City University of Hong Kong, Hong Kong. Nowadays, he is Lecturer in the Department of Technology, School of Science and Technology, The Open University of Hong Kong, Hong Kong. His current research interests include Statistical Process Monitoring, Data Mining and Generalized Linear Modelling.

Saddam Akber Abbasi obtained PhD degree in Statistics from The University of Auckland, New Zealand. He is currently working as an Associate Professor in Department of Mathematics, Statistics and Physics, Qatar University, Doha, Qatar. Before this, he worked in King Fahd University of Petroleum and Minerals, Dhahran, Saudi Arabia for three years. His research interests include Statistical Process Control, Non-parametric techniques and time series analysis.

How to cite this article: Mahmood T, Abbasi SA. Efficient monitoring of coefficient of variation with an application to chemical reactor process. *Qual Reliab Engng Int*. 2021;37:1135–1149. https://doi.org/10.1002/qre.2785